Special Feature: Vehicle Engineering

Research Report

Clarification and Achievement of Theoretical Limitation in Vehicle Dynamics Integrated Management

Eiichi Ono, Yoshikazu Hattori, Hiroaki Aizawa, Hiroaki Kato, Shinichi Tagawa and Satoru Niwa

Report received on Sep. 26, 2012

ABSTRACT In this article, a vehicle dynamics integrated control algorithm using an on-line nonlinear optimization method is proposed for 4-wheel distributed steering and 4-wheel distributed traction/braking systems. The proposed distribution algorithm calculates the magnitude and direction of tire forces that satisfy constraints corresponding to the target resultant force and moment of vehicle motion and also minimizes the maximum μ rate (= tire force / friction circle) of each tire. The convexity of this problem is shown, and so global optimality of the convergent solution of the recursive algorithm is guaranteed. This implies that the theoretical limited performance of vehicle dynamics integrated control is clarified. The proposed algorithm is based on SQP (Sequential Quadratic Programming) and the steepest gradient algorithm. Calculation performance of the proposed algorithm is compared that of the primal-dual interior-point method, which is a representative optimization method. Furthermore, the effect of this vehicle dynamics control is demonstrated by a simulation and experiment comparing various vehicle dynamics integrated control methods.

KEYWORDS Automobile, Maneuverability, Optimal Control, Nonlinear Dynamics, Vehicle Dynamics Integrated Management, 4-Wheel Distributed Steering, 4-Wheel Distributed Traction/Braking

1. Introduction

The motion of a vehicle in the three degrees of freedom (forward/back, lateral, yaw) is controlled by the steering and traction/braking forces from the four tires. If each of the tires can be individually steered and operated for traction/braking, the task of control grows from three control inputs (forward/back, lateral, yaw) to eight, providing redundancy to the system. Vehicles move using the friction between the tires and the ground. The frictional forces at the tires have limits dependent on the conditions of the road surface. These limits are called the friction circle, and a tire cannot exert any force on the roadway in excess of the friction circle. To extend the limits of the performance of a car, it is necessary to ensure that the forces exerted by all tires work efficiently in cooperation with each other. The problem of integrated control of vehicle motion then becomes how to best use the redundant degrees of freedom. Since the friction circle constitutes nonlinear limiting conditions due to the limitations on the frictional forces at each wheel, the share of the forward or back and lateral forces and the yaw moment (vehicle forces and moments) exerted by each tire to obtain the intended motion becomes a nonlinear problem.(1) The most common approach to the solution of this nonlinear problem has been to adapt empirical knowledge,(2-4) but in recent years, other methods which formulate the problem as a mathematical optimization problem have been advocated.(5-7) Mokhimar et al.(5) have proposed using the sum of the squares of the workload of the tires (tire μ rate × friction coefficient at the road surface) as an index to be minimized in 4-wheel steering and 4-wheel drive. Nishihara et al.(6) solved the min-max problem for minimizing the tire load under the worst possible loads with respect to the friction circle. This formulation allows us to estimate the maximum value of the tire μ rate, and the evaluation function constrains all of the forces exerted by the tires within the friction circle (tire μ rate is ≤ 1). The calculation load is far higher under this optimization scheme than under Mokhimar et al.'s formulation, but it predicts the yaw moment due to the

Reprinted from Transactions of the Japan Society of Mechanical Engineers. Series C (in Japanese), Vol. 73, No. 729, pp. 1425-1432,

forward/back force separately from the yaw moment due to the lateral force at each wheel, and thus, allows the problem to be simplified. It is a key to simplifying the problem, but it poses limitations on optimizing the tire μ rate. It would be preferable to devise a different integrated control scheme eliminating those limitations, i.e., a more efficient scheme for further lowering the tire μ rate. Ono et al.(7) noted that the solution of the min-max problem for μ was a weighted solution in nearly all cases, and proposed a method that included weighted tire μ rates in the constraints. Not only does this procedure guarantee minimizing the tire μ rate in nearly all regions, the number of parameters to be optimized is cut in half, so it also reduces the calculation load. Still, sometimes, depending on the actual vehicle forces and moment balance, the provided solution to the min-max problem for the tire μ rate does not represent a weighted solution.

This paper proposes an algorithm based on the tire μ rate weighting control algorithm of Ono et al.(7) that searches for fractions of the tire μ rate with respect to the upper limit of the μ rate for each vehicle tire. This load-distributing algorithm derives an analytical solution that minimizes the upper limit of the μ rate for each tire and enables the control system to achieve the theoretical limit of the integrated control of steering and thrust at all four tires.

2. Optimization Problem

2. 1 Formulation of the Problem

The vehicle model is described with the coordinates shown in **Fig. 1**, in which the X-axis is the longitudinal

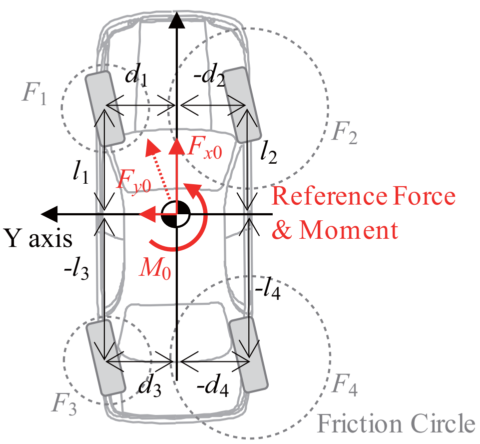

Fig. 1 Vehicle model and coordinates.

direction of the vehicle and the Y-axis is perpendicular to the X-axis. On the assumption that a magnitude F_i (in this case, $i = 1, 2, 3, 4$, where 1: left front wheel, 2: right front wheel, 3: left rear wheel, 4: right rear wheel) of a friction circle in each of the wheels (i.e., each wheel friction circle) is known, the direction of the generating force of each wheel tire and a μ rate (= tire force / friction circle) in each of the wheels can be determined to minimize the upper limit value (the maximum value in four wheels) of the μ rate (= tire force / friction circle) in each wheel, while securing the target vehicle body force (a longitudinal force F_{x0}, a lateral force F_{y0}) and target yaw moment M_{z0}. Further, the tire force in each of the wheels can be described as follows, on the assumption that the upper limit of the μ rate in each of the wheels is set to γ, a percentage indicating the ratio of the μ rate in each wheel with respect to the upper limit γ of the μ rate is set to r_i, and the tire generating force direction in each wheel is set to q_i:

$$F_{xi} = \gamma r_i F_i \cos q_i, \quad \cdots\cdots (1)$$

$$F_{yi} = \gamma r_i F_i \sin q_i. \quad \cdots\cdots (2)$$

By describing the position of each tire as $(x, y) = (l_i, d_i)$, as shown in Fig. 1, the vehicle body force and the yaw moment can be described by the following constraint condition.

$$\gamma \sum_{i=1}^{4} r_i F_i \cos q_i = F_{x0} \quad \cdots\cdots (3)$$

$$\gamma \sum_{i=1}^{4} r_i F_i \sin q_i = F_{y0} \quad \cdots\cdots (4)$$

$$\gamma \sum_{i=1}^{4} r_i F_i \left(-d_i \cos q_i + l_i \sin q_i\right) = M_{z0} \quad \cdots\cdots (5)$$

By eliminating γ from equations (3)-(5), the constraints of q_i can be obtained as

$$\sum_{i=1}^{4} r_i F_i \left(\frac{-d_i F_{x0} - d_i F_{y0} - F_{y0} - M_{z0}}{M_{F0}} \cos q_i + \frac{l_i F_{x0} + l_i F_{y0} + F_{x0} - M_{z0}}{M_{F0}} \sin q_i \right) = 0 , \quad \cdots\cdots (6)$$

$$\sum_{i=1}^{4} r_i F_i \left\{ \frac{M_{z0}\left(d_0^2 F_{x0} - d_i M_{z0}\right) + d_i M_{F0}^2}{M_{F0}^2} \cos q_i + \frac{M_{z0}\left(l_0^2 F_{y0} + l_i M_{z0}\right) - l_i M_{F0}^2}{M_{F0}^2} \sin q_i \right\} = 0 , \quad \cdots (7)$$

where

$$d_0 = \sum_{i=1}^{4} \frac{|d_i|}{4} , \quad \cdots (8)$$

$$l_0 = \sum_{i=1}^{4} \frac{|l_i|}{4} , \quad \cdots (9)$$

$$M_{F0} \equiv \sqrt{\left(d_0 F_{x0}\right)^2 + \left(l_0 F_{y0}\right)^2 + M_{z0}^2} . \quad \cdots (10)$$

M_{F0} is a value for normalizing constraints (6), (7) to improve the precision of the computation.

Performance function J, which minimizes the upper limit γ of the μ rate, is defined as the following formula (11):

$$J = \frac{\left(d_0 F_{x0}\right)^2 + \left(l_0 F_{y0}\right)^2 + M_{z0}^2}{\gamma} = \frac{M_{F0}^2}{\gamma} . \quad \cdots (11)$$

Since M_{F0} is a constant value, maximizing J implies minimizing γ. By substituting (3)-(5) into (11), the performance function can be rewritten as

$$J = \sum_{i=1}^{4} r_i F_i \left\{ \left(d_0^2 F_{x0} - d_i M_{z0}\right) \cos q_i + \left(l_0^2 F_{y0} + l_i M_{z0}\right) \sin q_i \right\} . \quad \cdots (12)$$

Then, the optimization problem is formulated as follows.

Problem 1: Finding q_i ($-\pi \leqq q_i \leqq \pi$), r_i ($0 \leqq r_i \leqq 1$) which maximizes performance function (12) with constraint equations (6) and (7).

2. 2 Search on a Fixed μ Rate Distribution

Since solutions of the min-max problem of the μ rate almost coincide with the equalized μ rate solutions,[7] we propose an optimization algorithm that separately optimizes q_i and r_i.

In this section, we show that the proposed algorithm optimizes q_i by using SQP (Sequential Quadratic Programming) with the assumption that r_i is fixed. This means that the μ rate distribution of four wheels is fixed. It is known that SQP is one of the most effective methods of nonlinear optimization that guarantees local optimality.[8] SQP is a recursive algorithm which approximates the nonlinear optimization problem as a quadratic problem around the optimal solution calculated in the preceding step. The constraints are approximated by a first-order Taylor expansion, and the performance function is approximated by a second-order Taylor expansion. Then, the optimal solution of the quadratic problem (optimization of the second-order performance function with linear constraints) is calculated. The approximated performance function can be described as

$$J = \sum_{i=1}^{4} r_i F_i \left\{ -\frac{1}{2} X_{Di} \left(q_i - X_i\right)^2 + Y_i \right\}, \quad \cdots (13)$$

where

$$X_i = \frac{X_{Ni}}{X_{Di}}, \quad \cdots (14)$$

$$X_{Ni} = \left(d_0^2 F_{x0} - d_i M_{z0}\right)\left(q_{i0} \cos q_{i0} - \sin q_{i0}\right) + \left(l_0^2 F_{y0} + l_i M_{z0}\right)\left(q_{i0} \sin q_{i0} + \cos q_{i0}\right), \quad \cdots (15)$$

$$X_{Di} = \left(d_0^2 F_{x0} - d_i M_{z0}\right) \cos q_{i0} + \left(l_0^2 F_{y0} + l_i M_{z0}\right) \sin q_{i0}, \quad \cdots (16)$$

$$Y_i = \left(d_0^2 F_{x0} - d_i M_{z0}\right) \cdot \left\{ \left(1 - \frac{q_{i0}^2}{2}\right) \cos q_{i0} + q_{i0} \sin q_{i0} \right\} + \left(l_0^2 F_{y0} + l_i M_{z0}\right) \left\{ \left(1 - \frac{q_{i0}^2}{2}\right) \sin q_{i0} - q_{i0} \cos q_{i0} \right\} + \frac{X_{Ni}^2}{2 X_{Di}} . \quad \cdots (17)$$

Furthermore, by using the variable transformation

$$p_i = \sqrt{r_i F_i X_{Di}}\left(q_i - X_i\right), \quad \cdots\cdots (18)$$

(13) can be rewritten as an Euclidian norm minimization problem of $\boldsymbol{p}$ as

$$J = \sum_{i=1}^{4}\left(-\frac{1}{2}p_i^2 + r_i F_i Y_i\right) = -\frac{1}{2}\|\mathbf{p}\|^2 + \sum_{i=1}^{4} r_i F_i Y_i\,, \quad \cdots\cdots (19)$$

where $\boldsymbol{p} = [p_1\ \ p_2\ \ p_3\ \ p_4]^T$.
The linearly approximated constraints can be described as

$$\begin{bmatrix} A_{11} & A_{12} & A_{13} & A_{14} \\ A_{21} & A_{22} & A_{23} & A_{24} \end{bmatrix}\boldsymbol{p} = \begin{bmatrix} B_1 \\ B_2 \end{bmatrix}, \quad \cdots\cdots (20)$$

where

$$A_{1i} = \sqrt{\frac{r_i F_i}{X_{Di}}}\cdot\left(\frac{d_i F_{x0} + d_i F_{y0} + F_{y0} + M_{z0}}{M_{F0}}\sin q_{i0} + \frac{l_i F_{x0} + l_i F_{y0} + F_{x0} - M_{z0}}{M_{F0}}\cos q_{i0}\right), \quad \cdots\cdots (21)$$

$$A_{2i} = \sqrt{\frac{r_i F_i}{X_{Di}}}\cdot\left\{-\frac{M_{z0}\left(d_0^2 F_{x0} - d_i M_{z0}\right) + d_i M_{F0}^2}{M_{F0}^2}\sin q_{i0} + \frac{M_{z0}\left(l_0^2 F_{y0} + l_i M_{z0}\right) - l_i M_{F0}^2}{M_{F0}^2}\cos q_{i0}\right\}, \quad \cdots\cdots (22)$$

$$B_1 = \sum_{i=1}^{4} r_i F_i\left[\frac{d_i F_{x0} + d_i F_{y0} + F_{y0} + M_{z0}}{M_{F0}}\cdot\left\{\left(q_{i0} - X_i\right)\sin q_{i0} + \cos q_{i0}\right\} + \frac{l_i F_{x0} + l_i F_{y0} + F_{x0} - M_{z0}}{M_{F0}}\cdot\left\{\left(q_{i0} - X_i\right)\cos q_{i0} - \sin q_{i0}\right\}\right], \quad \cdots\cdots (23)$$

$$B_2 = \sum_{i=1}^{4} r_i F_i\left[-\frac{M_{z0}\left(d_0^2 F_{x0} - d_i M_{z0}\right) + d_i M_{F0}^2}{M_{F0}^2}\cdot\left\{\left(q_{i0} - X_i\right)\sin q_{i0} + \cos q_{i0}\right\} + \frac{M_{z0}\left(l_0^2 F_{y0} + l_i M_{z0}\right) - l_i M_{F0}^2}{M_{F0}^2}\cdot\left\{\left(q_{i0} - X_i\right)\cos q_{i0} - \sin q_{i0}\right\}\right]. \quad \cdots\cdots (24)$$

An Euclidian norm minimum solution satisfying (20) can be determined as

$$\boldsymbol{p} = \begin{bmatrix} A_{11} & A_{12} & A_{13} & A_{14} \\ A_{21} & A_{22} & A_{23} & A_{24} \end{bmatrix}^{\dagger}\cdot\begin{bmatrix} B_1 \\ B_2 \end{bmatrix}. \quad \cdots\cdots (25)$$

In this case, $A^{\dagger}$ is the pseudo-inverse matrix of matrix A. Then, $\boldsymbol{q}$, which expresses the tire force direction in each of the wheels, may be expressed as

$$\boldsymbol{q} = diag\left[\frac{1}{\sqrt{r_1 F_1 X_{D1}}}\quad \frac{1}{\sqrt{r_2 F_2 X_{D2}}}\quad \frac{1}{\sqrt{r_3 F_3 X_{D3}}}\quad \frac{1}{\sqrt{r_4 F_4 X_{D4}}}\right]\cdot\begin{bmatrix} A_{11} & A_{12} & A_{13} & A_{14} \\ A_{21} & A_{22} & A_{23} & A_{24} \end{bmatrix}^{\dagger}\cdot\begin{bmatrix} B_1 \\ B_2 \end{bmatrix} + \begin{bmatrix} X_1 \\ X_2 \\ X_3 \\ X_4 \end{bmatrix}, \quad \cdots\cdots (26)$$

where $\boldsymbol{q} = [q_1\ \ q_2\ \ q_3\ \ q_4]^T$.
Furthermore, a penalty function

$$P = \frac{1}{J} + \rho\left(|J_1| + |J_2|\right) \quad \cdots\cdots (27)$$

is defined, where

$$J_1 = \sum_{i=1}^{4} r_i F_i\left(\frac{-d_i F_{x0} - d_i F_{y0} - F_{y0} - M_{z0}}{M_{F0}}\cos q_i + \frac{l_i F_{x0} + l_i F_{y0} + F_{x0} - M_{z0}}{M_{F0}}\sin q_i\right), \quad \cdots\cdots (28)$$

$$J_2 = \sum_{i=1}^{4} r_i F_i \left\{ \frac{M_{z0}\left(d_0{}^2 F_{x0} - d_i M_{z0}\right) + d_i M_{F0}{}^2}{M_{F0}{}^2} \cos q_i + \frac{M_{z0}\left(l_0{}^2 F_{y0} + l_i M_{z0}\right) - l_i M_{F0}{}^2}{M_{F0}{}^2} \sin q_i \right\}, \quad \cdots\cdots (29)$$

and ρ in (27) is a positive constant. In the case that the penalty function (27) is computed by using the tire force direction q_i of each wheel, as derived by (26), and penalty function P is reduced, a convergence computation is carried out a recursive method repeatedly executing the computation of (14)-(16), (21)-(24) and (26).

2. 3 Search of μ Rate Distribution

In this section, the proposed algorithm optimizes r_i by using the steepest gradient method. When each wheel using percentage r_i with respect to the upper limit of the μ rate in each wheel is changed to $r_i + dr_i$, it is necessary to correct $\boldsymbol{q}$ in (26), for example, to $\boldsymbol{q} + d\boldsymbol{q}$, to satisfy the constraint condition of the target vehicle body force and moment. The changed amount $d\boldsymbol{q}$ of $\boldsymbol{q}$ expressing each wheel tire force direction is expressed as

$$d\boldsymbol{q} = diag\left[\frac{1}{\sqrt{r_1 F_1 X_{D1}}} \quad \frac{1}{\sqrt{r_2 F_2 X_{D2}}} \quad \frac{1}{\sqrt{r_3 F_3 X_{D3}}} \quad \frac{1}{\sqrt{r_4 F_4 X_{D4}}}\right] \cdot \begin{bmatrix} A_{11} & A_{12} & A_{13} & A_{14} \\ A_{21} & A_{22} & A_{23} & A_{24} \end{bmatrix}^{\dagger} \cdot \begin{bmatrix} \Delta_1(d\mathbf{r}) \\ \Delta_2(d\mathbf{r}) \end{bmatrix}, \quad \cdots\cdots (30)$$

where

$$\Delta_1(d\boldsymbol{r}) = -\sum_{i=1}^{4} dr_i F_i \cdot \left(\frac{-d_i F_{x0} - d_i F_{y0} - F_{y0} - M_{z0}}{M_{F0}} \cos q_i + \frac{l_i F_{x0} + l_i F_{y0} + F_{x0} - M_{z0}}{M_{F0}} \sin q_i \right), \quad \cdots\cdots (31)$$

$$\Delta_2(d\boldsymbol{r}) = -\sum_{i=1}^{4} dr_i F_i \cdot \left\{ \frac{M_{z0}\left(d_0{}^2 F_{x0} - d_i M_{z0}\right) + d_i M_{F0}{}^2}{M_{F0}{}^2} \cos q_i + \frac{M_{z0}\left(l_0{}^2 F_{y0} + l_i M_{z0}\right) - l_i M_{F0}{}^2}{M_{F0}{}^2} \sin q_i \right\}. \quad \cdots\cdots (32)$$

This case only satisfies the constraint condition of the target vehicle body force and moment; the correction is not fixed. In other words, infiniteness of the correcting methods may be provided; however, for simplifying the computation, we employ a correcting method utilizing the derived pseudo-inverse matrix as it is. In this case, the performance function J in (12) is changed to $J + dJ$. The change amount dJ can be expressed as

$$dJ = \sum_{i=1}^{4}\Big[dr_i F \cdot \left\{\left(d_0{}^2 F_{x0} - d_i M_{z0}\right)\cos q_i\right\}_i + \left(l_0{}^2 F_{y0} + l_i M_{z0}\right)\sin q_i\Big\}_i + r_i F_i dq_i \cdot \left\{ -\left(d_0{}^2 F_{x0} - d_i M_{z0}\right)\sin q_i + \left(l_0{}^2 F_{y0} + l_i M_{z0}\right)\cos q_i \right\}\Big]. \quad \cdots\cdots (33)$$

Then, the following equation can be derived by approximation.

$$\frac{\partial J}{\partial r} = \begin{bmatrix} F_1\left\{\left(d_0{}^2 F_{x0} - d_1 M_{z0}\right)\cos q_1 + \left(l_0{}^2 F_{y0} + l_1 M_{z0}\right)\sin q_1\right\} \\ F_2\left\{\left(d_0{}^2 F_{x0} - d_2 M_{z0}\right)\cos q_2 + \left(l_0{}^2 F_{y0} + l_2 M_{z0}\right)\sin q_2\right\} \\ F_3\left\{\left(d_0{}^2 F_{x0} - d_3 M_{z0}\right)\cos q_3 + \left(l_0{}^2 F_{y0} + l_3 M_{z0}\right)\sin q_3\right\} \\ F_4\left\{\left(d_0{}^2 F_{x0} - d_4 M_{z0}\right)\cos q_4 + \left(l_0{}^2 F_{y0} + l_i M_{z0}\right)\sin q_4\right\} \end{bmatrix} + \left(\begin{bmatrix} A_{11} & A_{12} & A_{13} & A_{14} \\ A_{21} & A_{22} & A_{23} & A_{24} \end{bmatrix}^{\dagger} \cdot \begin{bmatrix} D_{11} & D_{12} & D_{13} & D_{14} \\ D_{21} & D_{22} & D_{23} & D_{24} \end{bmatrix} \right)^T \cdot \begin{bmatrix} \sqrt{\frac{r_1 F_1}{X_{D1}}}\left\{-\left(d_0{}^2 F_{x0} - d_1 M_{z0}\right)\sin q_1 + \left(l_0{}^2 F_{y0} + l_1 M_{z0}\right)\cos q_1\right\} \\ \sqrt{\frac{r_2 F_2}{X_{D2}}}\left\{-\left(d_0{}^2 F_{x0} - d_2 M_{z0}\right)\sin q_2 + \left(l_0{}^2 F_{y0} + l_2 M_{z0}\right)\cos q_2\right\} \\ \sqrt{\frac{r_3 F_3}{X_{D3}}}\left\{-\left(d_0{}^2 F_{x0} - d_3 M_{z0}\right)\sin q_3 + \left(l_0{}^2 F_{y0} + l_3 M_{z0}\right)\cos q_3\right\} \\ \sqrt{\frac{r_4 F_4}{X_{D4}}}\left\{-\left(d_0{}^2 F_{x0} - d_4 M_{z0}\right)\sin q_4 + \left(l_0{}^2 F_{y0} + l_4 M_{z0}\right)\cos q_4\right\} \end{bmatrix} \quad \cdots\cdots (34)$$

where

$$D_{1i} = -F_i\left(\frac{-d_iF_{x0} - d_iF_{y0} - F_{y0} - M_{z0}}{M_{F0}}\cos q_i + \frac{l_iF_{x0} + l_iF_{y0} + F_{x0} - M_{z0}}{M_{F0}}\sin q_i\right), \quad (35)$$

$$D_{2i} = -F_i\left\{\frac{M_{z0}\left(d_0^{\,2}F_{x0} - d_iM_{z0}\right) + d_iM_{F0}^{\,2}}{M_{F0}^{\,2}}\cos q_i + \frac{M_{z0}\left(l_0^{\,2}F_{y0} + l_iM_{z0}\right) - l_iM_{F0}^{\,2}}{M_{F0}^{\,2}}\sin q_i\right\}. \quad (36)$$

Each wheel using percentage r_i with respect to the upper limit of the μ rate in each of the wheels is changed to

$$\boldsymbol{r} = \begin{cases} 0 & \left(\boldsymbol{r}_0 + k\dfrac{\partial J}{\partial \boldsymbol{r}} < 0\right) \\ \boldsymbol{r}_0 + k\dfrac{\partial J}{\partial \boldsymbol{r}} & \left(0 \le \boldsymbol{r}_0 + k\dfrac{\partial J}{\partial \boldsymbol{r}} \le 1\right) \\ 1 & \left(\boldsymbol{r}_0 + k\dfrac{\partial J}{\partial \boldsymbol{r}} > 1\right) \end{cases} \quad (37)$$

by using the steepest gradient method, before proceeding to the next step of the repeated computation. In (37), $\boldsymbol{r}_0$ denotes the previous value of $\boldsymbol{r}$ in the repeated computation, and k denotes a positive constant. Accordingly, in the case that performance function J is changed to become enlarged, $\boldsymbol{r}$ is corrected to become smaller.

Then, the upper limit γ of the μ rate can be derived from (11) and (12) with $\boldsymbol{r}$ and $\boldsymbol{q}$, which are calculated from (30) and (37), as

$$\gamma = \frac{\left(d_0F_{x0}\right)^2 + \left(l_0F_{y0}\right)^2 + M_{z0}^{\,2}}{\sum_{i=1}^{4} r_iF_i\left\{\left(d_0^{\,2}F_{x0} - d_iM_{z0}\right)\cos q_i + \left(l_0^{\,2}F_{y0} + l_iM_{z0}\right)\sin q_i\right\}}. \quad (38)$$

If the calculated γ by (38) is greater than 1, the resultant force and moment are restricted to

$$F_{x0rest} = \frac{F_{x0}}{\gamma}, F_{y0rest} = \frac{F_{y0}}{\gamma} M_{z0rest} = \frac{M_{z0}}{\gamma} \quad (39)$$

2. 4 Global Optimality

By using variable transformation with

$$x_i = r_i \cos q_i, \quad (40)$$

$$y_i = r_i \sin q_i, \quad (41)$$

problem 1 can be rewritten as the following problem

Problem 2: Finding x_i, y_i which maximizes the performance function

$$J = \sum_{i=1}^{4} F_i \cdot \left\{\left(d_0^{\,2}F_{x0} - d_iM_{z0}\right)x_i + \left(l_0^{\,2}F_{y0} + l_iM_{z0}\right)y_i\right\} \quad (42)$$

with the following constraint equations

$$\sum_{i=1}^{4} F_i\left(\frac{-d_iF_{x0} - d_iF_{y0} - F_{y0} - M_{z0}}{M_{F0}}x_i + \frac{l_iF_{x0} + l_iF_{y0} + F_{x0} - M_{z0}}{M_{F0}}y_i\right) = 0, \quad (43)$$

$$\sum_{i=1}^{4} F_i\left\{\frac{M_{z0}\left(d_0^{\,2}F_{x0} - d_iM_{z0}\right) + d_iM_{F0}^{\,2}}{M_{F0}^{\,2}}x_i + \frac{M_{z0}\left(l_0^{\,2}F_{y0} + l_iM_{z0}\right) - l_iM_{F0}^{\,2}}{M_{F0}^{\,2}}y_i\right\} = 0, \quad (44)$$

$$x_i^2 + y_i^2 \le 1. \quad (45)$$

Problem 2 is clearly a convex problem, and so problem 1 is also a convex problem. Then, the proposed algorithm guarantees global optimality of the convergent point. This means that the proposed algorithm achieves the theoretical limitation of the vehicle force and moment when γ calculated by (38) is greater than 1.

3. Benchmark

3. 1 Achievement of Theoretical Limitation

This section shows the efficiency of the proposed algorithm, which achieves the theoretical limitation of a vehicle force and moment, by comparing it with general quadratic programming. We consider the following minimization problem of the sum of squares of the μ rate as a benchmark; this is an extended problem of Mokhiamar and Abe.[5]

Problem 3: Finding F_{xi}, F_{yi} which maximizes the performance function

$$J = \sum_{i=1}^{4}\left(\frac{F_{xi}^{\ 2} + F_{yi}^{\ 2}}{F_i^2}\right) \quad (46)$$

with constraint equations

$$\sum_{i=1}^{4} F_{xi} = F_{x0}, \quad (47)$$

$$\sum_{i=1}^{4} F_{yi} = F_{y0}, \quad (48)$$

$$\sum_{i=1}^{4}\left(-d_i F_{xi} + l_i F_{yi}\right) = M_{z0}. \quad (49)$$

The solution of problem 3 can be calculated by using variable transformation and the pseudo-inverse matrix, as shown in Section 2.2. In this section, the generated vehicle longitudinal forces are compared for straight-line braking (F_{y0} = 0 N, M_{z0} = 0 Nm) on a split μ road (μ = 1.0, 0.2).

Figure 2 shows the tire forces of a vehicle controlled by the proposed method and a vehicle controlled by quadratic programming. Both of the controls achieve the reference braking force within a moderate area when the reference braking force = 7,000 N. However, the vehicle controlled by quadratic programming cannot achieve the reference braking force in the critical region when the reference braking force = 10,000 N, even though the vehicle controlled by the proposed method can. **Figure 3** shows the relation between the reference braking force and μ rate in each wheel. The μ rate of the front left wheel, which has the largest friction circle, indicates a large value compared with that of the other wheels, when the vehicle is controlled by quadratic programming, which minimizes the sum of square μ rates. Then, the μ rate

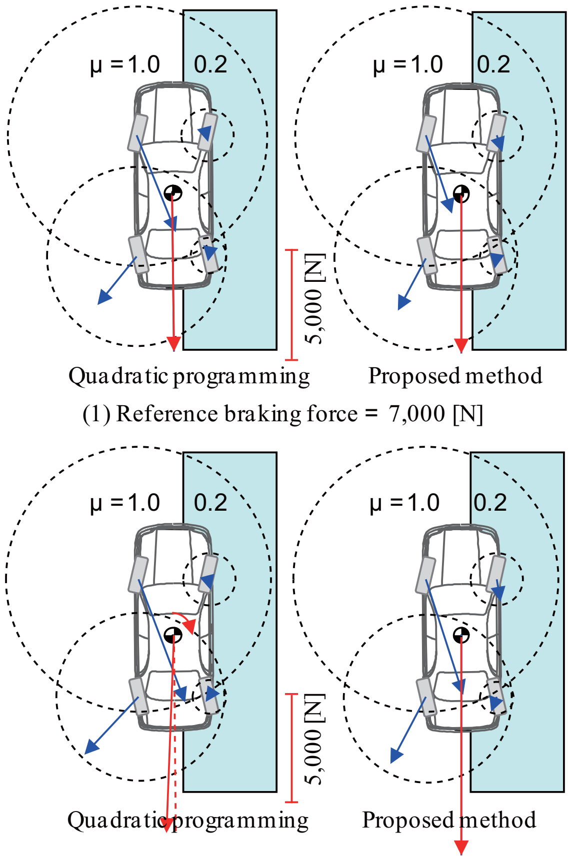

Fig. 2 Straight-line braking on split μ road.

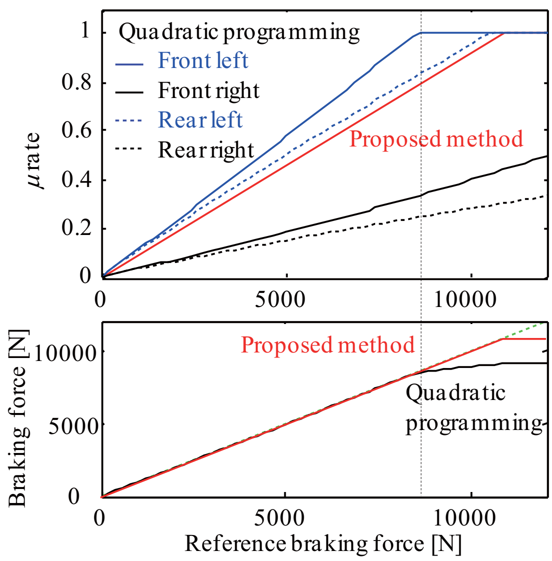

Fig. 3 Relation between reference braking force and μ rate.

of the front left wheel is saturated first, so that subsequent reference vehicle force and moment cannot be achieved. In contrast, the proposed method, which minimizes the upper limit of the μ rate, calculates the equalized μ rate solutions, and provides high performance in the critical region.

3. 2 Calculation of the Optimization

As shown in Section 2.4, problem 1 is a convex problem, so the problem can be transformed to second-order cone programming (SOCP). The primal-dual interior-point method is a powerful method for SOCP. The calculation speed of the proposed algorithm is shown in comparison with the primal-dual interior-point method, which is a representative optimization method.

Here, the nonlinear constraint

$$x_i^2 + y_i^2 \le 1, \quad \cdots\cdots (45)$$

in problem 2 can be extended to a second-order cone constraint and linear constraint, as follows.

$$\sqrt{x_i^2 + y_i^2} \le z_i \quad \cdots\cdots (50)$$

$$z_i = 1 \quad \cdots\cdots (51)$$

Figure 4 shows the relation between the calculation time and accuracy of solutions using the proposed method and primal-dual interior-point method under the condition of straight-line braking on a split μ road, as shown in Section 3.1. The penalty function indicates

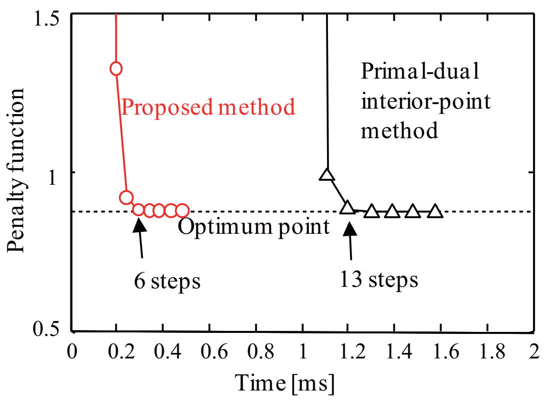

Fig. 4 Relation between calculation time and accuracy (Pentium M 900 MHz).

(27) with $\rho = 1$, and it shows an error in the constraint and performance function ($1/J$). The proposed method improves calculation efficiency by the optimization algorithm that separately optimizes q_i and r_i. This is based on the viewpoint that solutions of the min-max problem of the μ rate almost coincide with the equalized μ rate solutions. Then, the solution of the proposed method almost converges to the optimum point in six steps. In contrast, the calculation time of the primal-dual interior-point method, which applies to the extended problem with constraints (50) and (51), is four times that of the proposed method.

4. Experimental Results

In this paper, a vehicle with 4-wheel distributed steering and 4-wheel distributed traction/braking system is assumed, and the steer angle of each wheel is calculated from the brush model[(11)] as

$$\delta_i = \beta + \frac{l_i r}{u} - \tan^{-1}\left(\frac{K_s}{K_\alpha}\frac{-\kappa_i \sin q_i}{1-\kappa_i \cos q_i}\right), \quad \cdots\cdots (52)$$

where

$$\kappa_i = \frac{3F_i}{K_s}\left\{1-(1-r_i\gamma)^{\frac{1}{3}}\right\}, \quad \cdots\cdots (53)$$

K_s is the braking stiffness, K_α is the cornering stiffness, β is the vehicle slip angle, r is the yaw velocity, and u is the vehicle longitudinal velocity. In this section, the proposed method is applied to the active front and rear steering vehicle to demonstrate the high performance of the distribution algorithm, which achieves the theoretical limited performance. In other words, the steer angle is controlled to a mean value of the right and left reference calculated by (52).

Figure 5 shows the experimental results of straight-line braking ($F_{y0} = 0$ N, $M_{z0} = 0$ Nm) on a split μ road (μ = 1.0, 0.2). As a comparison, an ABS (anti-lock brake system) vehicle without steering control and the integrated control vehicle with active front steering system[(12)] are also shown in Fig. 5. The driver driving the ABS vehicle use the steering wheel to stabilize the vehicle. In contrast, the vehicle with active front steering and the proposed method can apply straight-line braking without using the steering wheel. Furthermore, the proposed method shows a high performance compared with the vehicle with active front steering. **Figure 6** shows the tire forces of the proposed method. The experimental tire forces are measured by using a wheel dynamometer. This figure also shows a theoretical solution assuming a 4-wheel distributed steering system with high braking performance (94%).

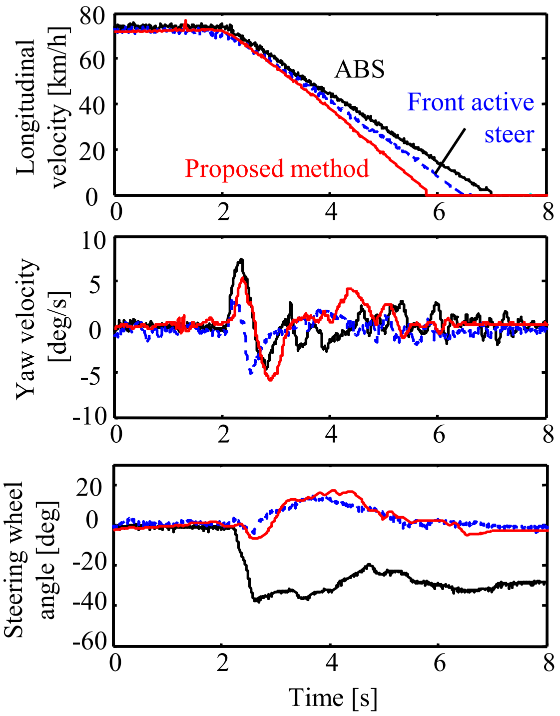

Fig. 5 Experimental results of straight-line braking on split μ road (μ = 0.2, 1.0).

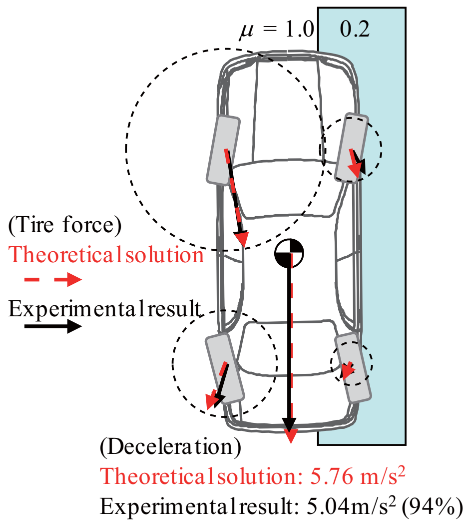

Fig. 6 Tire forces of straight-line braking on split μ road.

5. Conclusions

This paper proposes a distribution algorithm of the vehicle tire forces for 4-wheel distributed steering and 4-wheel distributed traction/braking systems. The proposed distribution algorithm minimizes the maximum μ rate of each tire with constraints corresponding to the target resultant force and moment of vehicle motion. Convexity of this problem is shown, and so global optimality of the convergent solution of the recursive algorithm is guaranteed. This implies that the theoretical limited performance of vehicle dynamics integrated control is clarified. The calculation speed of the proposed algorithm is shown in comparison with that of the primal-dual interior-point method, which is a representative optimization method. In addition, the effect of the proposed vehicle dynamics control is demonstrated by a simulation and experiment to compare it with other vehicle dynamics integrated control methods.

References

(1) Hattori, Y., et al., "Force and Moment Control with Nonlinear Optimum Distribution for Vehicle Dynamics", *Proceedings of the 6th International Symposium on Advanced Vehicle Control* (2002), pp. 595-600, JSAE.

(2) Gordon, T. J., et al., "Integrated Control Methodologies for Road Vehicles", *Journal of Vehicle System Dynamics*, Vol. 40, No. 1-3 (2003), pp. 157-190

(3) David, J. H., et al., "Integrated Chassis Control through Coordination of Active Front Steering and Intelligent Torque Distribution", *Proceedings of the 7th International Symposium on Advanced Vehicle Control* (2004), pp. 333-339, JSAE.

(4) Brandao, F. V., et al., "A Layered Approach to the Integrated Control of Longitudinal Wheel Slip and Vehicle Yaw Motion", *Proceedings of the 7th International Symposium on Advanced Vehicle Control* (2004), pp. 507-512, JSAE.

(5) Mokhimar, O. and Abe, M., "Effects of an Optimum Cooperative Chassis Control from the View Points of Tire Workload", *Proceedings of Society of Automotive Engineers of Japan Annual Congress*, No. 33-03 (2003), 20035448, pp. 15-20, JSAE.

(6) Nishihara, O., et al., "Optimization of Lateral and Driving/Braking Force Distribution of Independent Steering Vehicle (Minimax Optimization of Tire Workload)", *Transactions of the Japan Society of Mechanical Engineers. Series C* (in Japanese), Vol. 72, No. 714 (2006), pp. 537-544.

(7) Ono, E., et al., "Vehicle Dynamics Integrated Control

for Four-Wheel-Distributed Steering and Four-Wheel-Distributed Braking/Traction Systems", *Journal of Vehicle System Dynamics*, Vol. 44, No. 2 (2006), pp. 139-151.

(8) Yamakawa, H., *Handbook of Optimum Design* (in Japanese) (2003), pp.30-31, Asakura Publishing.

(9) Kodama, S. and Suda, N., *Matrix Theory for System Control* (in Japanese) (1978), pp. 332-347, The Society of Instrument and Control Engineers.

(10) Tamura, A. and Muramatsu, M., *Optimization Method* (in Japanese) (2002), pp. 166-195, *Kyoritu Syuppan*.

(11) Abe, M., *Vehicle Dynamics and Control* (in Japanese) (1992), pp. 30-39, *Sankaido*.

(12) Hattori, Y. and Koibuchi, K., "Integrated Control of Braking and Steering for Vehicle Dynamics", *The Society of Instrument and Control Engineers Transactions on Industrial Application* (in Japanese) Vol. 4, No. 11 (2005), pp. 75-80.

Eiichi Ono

Research Field:
- Vehicle Dynamics Control

Academic Degree: Dr.Eng.

Academic Societies:
- The Japan Society of Mechanical Engineers
- Society of Automotive Engineers of Japan
- The Society of Instrument and Control Engineers

Awards:
- SICE Award for Outstanding Paper, 1995
- IFAC Congress Applications Paper Prize, 2002
- Paper Award of AVEC, 2002
- Paper Award of AVEC, 2004
- JSME Medal for Outstanding Paper, 2007

Yoshikazu Hattori

Research Fields:
- Human-vehicle System and Application to Vehicle Dynamics Design
- Nonlinear Optimum Control
- Adaptive Control

Academic Degree: Dr.Eng.

Academic Societies:
- The Japan Society of Mechanical Engineers
- The Society of Instrument and Control Engineers
- The Institute of Systems, Control and Information Engineers
- Society of Automotive Engineers of Japan

Awards:
- Society of Automotive Engineers of Japan Technological Development Award, 2005
- SICE Award for Outstanding Paper, 2006

Hiroaki Aizawa*

Research Field:
- Vehicle Dynamics Control

Academic Society:
- Society of Automotive Engineers of Japan

Award:
- JSME Medal for Outstanding Paper, 2007

Hiroaki Kato**

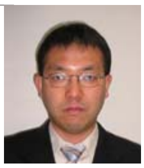

Research Field:
- Vehicle Dynamics Control

Academic Society:
- Society of Automotive Engineers of Japan

Award:
- JSME Medal for Outstanding Paper, 2007

Shinichi Tagawa*

Research Field:
- Vehicle Dynamics Control

Academic Society:
- Society of Automotive Engineers of Japan

Award:
- JSME Medal for Outstanding Paper, 2007

Satoru Niwa***

Research Field:
- Vehicle Dynamics Control

Academic Societies:
- The Japan Society of Mechanical Engineers
- Society of Automotive Engineers of Japan

Award:
- JSME Medal for Outstanding Paper, 2007

*AISIN SEIKI Co., Ltd.
**JTEKT Corporation
***Toyota Motor Corporation